

On linear dust-gas streaming instabilities in protoplanetary discs

Emmanuel Jacquet,¹ Steven Balbus,² Henrik Latter³

¹*LMCM, Muséum National d'Histoire Naturelle, 57 rue Cuvier, 75005 Paris, France*

²*LRA, Ecole Normale Supérieure, 45 rue d'Ulm, 75005 Paris, France*

³*AFD Group, DAMTP, University of Cambridge, CMS Wilberforce Rd, Cambridge UK CB3 0WA*

9 July 2018

ABSTRACT

We revisit, via a very simplified set of equations, a linear streaming instability (technically an overstability), which is present in, and potentially important for, dusty protoplanetary disks (Youdin and Goodman 2005). The goal is a better understanding of the physical origin of such instabilities, which are notoriously subtle. Rotational dynamics seem to be essential to this type of instability, which cannot be captured by one-dimensional Cartesian models. Dust ‘pileups’ in moving pressure maxima are an important triggering mechanism of the instability, and drag feedback of dust upon the gas allows these maxima to be strengthened. Coriolis forces and the background drift counteract the effects of the pressure force.

1 INTRODUCTION

The formation of planets via dust accretion starting with micron-sized grains and ending with $10^4 - 10^5$ -km-sized bodies in a protoplanetary disc is a multiphase process (see e.g. the review by Chiang and Youdin (2010), henceforth CY10). Grains smaller than roughly a centimetre coagulate via sticking (e.g. Dominik *et al.* 2007), while for the largest sizes, gravity of the planetary bodies plays a dominant role (e.g. Ida 2010).

Between these two limits, there is a gap that neither mechanism seems able to leapfrog. Beyond a size of 1 cm - 1 m, collisions occur at velocities of order $1 - 10 \text{ m s}^{-1}$. These lead either to fragmentation or to bouncing (Zsom *et al.* 2010), rather than to systematic aggregation. Worse yet, particles of this size will drift sunward at the dramatic rate of 1 AU per century (Weidenschilling 1977). This is because solids tend to orbit the Sun at the full Keplerian speed, while the gas moves slightly slower because of the support from an outward directed pressure force. Thus, the solids experience a headwind that removes angular momentum via gas drag. This effect is the cause of the “metre-size barrier”.

Self-gravity of the dust could in principle promote accretion past this barrier provided some process enhances the dust density. A classic scenario for this is one in which the vertical component of the Sun’s gravity causes sedimentation to the disc midplane and increases the dust density (Goldreich and Ward 1973). Although Weidenschilling (1980) had suggested that Kelvin-Helmholtz instabilities could prevent the Roche density from being reached, recent studies indicate that this is not an issue for discs a few times more massive than the minimum mass solar nebula, or with supersolar metallicities (e.g. Chiang 2008; Lee *et al.* 2010a,b). Moreover, Youdin (2011) showed that inclusion of gas drag could alleviate the need to actually reach

the Roche density. However, these mechanisms assume a low level of global turbulence. While the magnetorotational instability (Balbus and Hawley 1998) may be suppressed in the so-called dead zone (Gammie 1996), fluctuations arising from forced density waves or other instabilities could still be present (Fleming and Stone 2003; Lesur and Papaloizou 2010; Latter *et al.* 2010). Concentrating the dust is problematic.

However, interesting effects already occur as soon as the dust-to-gas ratio is of order unity, say around the mid-plane, or as a result of turbulent concentration (e.g. Cuzzi *et al.* 2003). This is because the dynamical back-reaction of the dust on the gas is then important, while self-gravity itself may still be negligible. In fact, Youdin and Goodman (2005) (hereafter YG05) discovered that the interpenetration of dust and gas in a Keplerian disc was linearly overstable: a process that they named the *streaming instability*, a convention we shall henceforth adopt. The dust particles can behave collectively via their interaction with the gas, leading to disordered flows that facilitate grain clumping—as witnessed by the numerical simulations of Youdin and Johansen (2007) (hereafter YJ07) and Johansen and Youdin (2007). Bai and Stone (2010) confirmed that in the nonlinear regime, dust densities up to three orders of magnitude above the background could be attained, which Johansen *et al.* (2007) argued would suffice to instigate gravitational clustering. As relatively large (10 cm - 1 m) particles are needed for significant clumping (Bai and Stone 2010), it remains to be demonstrated whether solids can have grown this large beforehand (Lee *et al.* 2010b).

Although much attention has been devoted to the streaming instability in the past years, its physical interpretation in the *linear* phase remains somewhat obscure. For example, as YJ07 point out, the idea that radial drift

slows down in overdense regions and leads to a sort of ‘traffic jam’, does not explain the onset of growth in the linear phase—such reasoning leads, in fact, to stable wave propagation. Such traffic jams, however, appear to be relevant for the non-linear phase (JY07). JY07 showed that drafting, analogous to pelotons in bicycle races, also was not necessary for the initial generation of particle overdensities, although it could enhance growth if present. CY10 discuss a one-dimensional vertically integrated toy model drawn from Goodman and Pindor (2000), in which a (single) fluid is subject to a “collective drag” acceleration in the sense that a drag coefficient depending upon the fluid density emerges from collective behavior. This system is found to be overstable. It is unclear, however, in what sense the streaming instability conforms to this notion of collective drag since it is local in nature: the equations are not vertically integrated and the drag acceleration does not depend *ab initio* on the density of the fluid acted upon.

We are therefore motivated to reconsider the origins of dust clumping. In this paper, we revisit the linear streaming instability. In §2, we review the basic equations leading to the YG05 results and propose, in an appropriate limit, a markedly reduced system in which the instability arises. We make the point in §3 that rotational dynamics are essential to understand the streaming instability. In §4, we propose an interpretation of the streaming instability. In §5, we summarise our conclusions.

2 STREAMING INSTABILITY AND REDUCED SYSTEMS

In this section, by way of establishing notation (largely that of YG05), we briefly review the fundamental equations along with some of their more important results. We then propose a significant reduction of the system of equations that involves two successive levels of approximation, yet still produces the streaming instability.

2.1 Fundamental two-fluid equations and local stability analysis

Let us model the dust as a collection of identical, indestructible spheres, of mass density ρ_p and velocity \mathbf{V}_p . The gas density and velocity, on the other hand, we denote by ρ_g and \mathbf{V}_g , respectively. Their evolution equations are (see Appendix A for justification of the dust equations):

$$\frac{\partial \rho_p}{\partial t} + \nabla \cdot (\rho_p \mathbf{V}_p) = 0 \quad (1)$$

$$\frac{\partial \rho_g}{\partial t} + \nabla \cdot (\rho_g \mathbf{V}_g) = 0 \quad (2)$$

$$\mathcal{D}_p \mathbf{V}_p = -\Omega^2 \mathbf{R} - \frac{\mathbf{V}_p - \mathbf{V}_g}{t_{\text{stop}}} \quad (3)$$

$$\mathcal{D}_g \mathbf{V}_g = -\Omega^2 \mathbf{R} + \frac{\rho_p}{\rho_g} \frac{\mathbf{V}_p - \mathbf{V}_g}{t_{\text{stop}}} - \frac{\nabla P}{\rho_g}, \quad (4)$$

where Ω is the Keplerian angular velocity, $\mathcal{D}_{p,g} \equiv \partial/\partial t + \mathbf{V}_{p,g} \cdot \nabla$ the particle/gas Lagrangian derivatives, and \mathbf{R} the

cylindrical vector radius. We ignore the vertical component of the solar gravity, as well as self-gravity.

The particle stopping time t_{stop} depends on the size and velocity regime (e.g. Weidenschilling 1977). For example, for particles that are both small compared to the gas mean-free-path and drifting subsonically relative to the gas (as appropriate, e.g., for chondrule-sized bodies at a few AUs in a Minimum Mass Solar Nebula), Epstein’s law (Epstein 1924) applies:

$$t_{\text{stop}} = \frac{\rho_s a}{\rho_g v_T}, \quad (5)$$

with $v_T = \sqrt{8k_B T / \pi m}$ (with m the molecular mass and T the temperature), roughly the sound speed, ρ_s the *internal* density of the grains (not to be confused with ρ_p) and a the grain radius. Regardless of the relevant drag law, one defines a dimensionless stopping time measuring the coupling of dust to dynamical disturbances:

$$\tau_s \equiv \Omega t_{\text{stop}}, \quad (6)$$

By virtue of Newton’s third law, an all-important feedback term of the dust on the gas appears in the Euler equation for the gas (4). The system of equations is closed by assuming gas incompressibility (the Boussinesq approximation), as in YG05.

It is convenient to express equations (1)–(4) in terms of centre-of-mass velocity $\mathbf{V} \equiv (\rho_p \mathbf{V}_p + \rho_g \mathbf{V}_g) / \rho$ (with $\rho \equiv \rho_p + \rho_g$ the total density) and the relative dust-to-gas drift $\Delta \mathbf{V} \equiv \mathbf{V}_p - \mathbf{V}_g$ (YG05):

$$\frac{\partial \rho}{\partial t} + \nabla \cdot (\rho \mathbf{V}) = 0 \quad (7)$$

$$\nabla \cdot (\mathbf{V} - \frac{\rho_p}{\rho} \Delta \mathbf{V}) = 0 \quad (8)$$

$$\frac{\partial \mathbf{V}}{\partial t} + \mathbf{V} \cdot \nabla \mathbf{V} + \mathbf{F}(\Delta \mathbf{V}^2) = -\Omega^2 \mathbf{R} - \frac{\nabla P}{\rho} \quad (9)$$

$$\frac{\partial \Delta \mathbf{V}}{\partial t} + \mathbf{V} \cdot \nabla (\Delta \mathbf{V}) + (\Delta \mathbf{V} \cdot \nabla) \mathbf{V} + \mathbf{G}(\Delta \mathbf{V}^2) = -\frac{\rho}{\rho_g} \frac{\Delta \mathbf{V}}{t_{\text{stop}}} + \frac{\nabla P}{\rho_g}, \quad (10)$$

with:

$$\mathbf{F}(\Delta \mathbf{V}^2) \equiv \frac{1}{\rho} \nabla \cdot \left(\frac{\rho_g \rho_p}{\rho} \Delta \mathbf{V} \Delta \mathbf{V} \right) \quad (11)$$

$$\mathbf{G}(\Delta \mathbf{V}^2) \equiv \frac{\rho_g}{\rho} \Delta \mathbf{V} \cdot \nabla \left(\frac{\rho_g}{\rho} \Delta \mathbf{V} \right) - \frac{\rho_p}{\rho} \Delta \mathbf{V} \cdot \nabla \left(\frac{\rho_p}{\rho} \Delta \mathbf{V} \right). \quad (12)$$

We shall now work in the so-called shearing-sheet approximation: We neglect all curvature terms and disc-scale gradients since the lengthscales of interest are much smaller than the heliocentric distance, or even the pressure scale height. We also adopt Cartesian coordinates in a frame corotating with the Keplerian flow at a fixed heliocentric distance R_0 , at angular velocity Ω . We denote by x , y and z coordinates in the radial, azimuthal, and vertical (that is, perpendicular to the midplane) directions, respectively, and \mathbf{e}_x , \mathbf{e}_y and \mathbf{e}_z the corresponding unit vectors.

Using this model, Nakagawa *et al.* (1986) computed the equilibrium solution to equations (7)–(10),

$$\mathbf{V} = \left(-\frac{g_e}{2\Omega} - \frac{3}{2} \Omega x \right) \mathbf{e}_y \quad (13)$$

$$\Delta \mathbf{V} = -\frac{g_e t_{\text{stop}}}{1 + (f_g \tau_s)^2} \mathbf{e}_x + \frac{f_g g_e \Omega t_{\text{stop}}^2}{2(1 + (f_g \tau_s)^2)} \mathbf{e}_y, \quad (14)$$

where $f_{g,p} \equiv \rho_{g,p}/\rho$ the mass fraction of gas and particles (of uniform densities in this equilibrium flow), and

$$g_e \equiv -\frac{1}{\rho} \frac{dP}{dR} \quad (15)$$

is the pressure-induced acceleration on the gas+dust fluid. It is the free energy stored in this gradient that the streaming instability can access (YG05). This gradient, consequently, introduces a lengthscale which helps determine the characteristic scale of the instability. We denote this scale by L and quantify it through:

$$L = \frac{g_e}{\Omega^2} \sim \left(\frac{H}{R}\right) H, \quad (16)$$

where H is the gas disc semi-thickness. It follows that L is a small fraction of H .

We now decompose the variables in equilibrium value and perturbation as follows:

$$\mathbf{V} = \mathbf{V}_0 + \mathbf{v} \quad (17)$$

$$\Delta \mathbf{V} = \Delta \mathbf{V}_0 + \Delta \mathbf{v} \quad (18)$$

$$\rho = \rho_0(1 + \delta) \quad (19)$$

$$P = P_0(x) + \rho_0 h, \quad (20)$$

where the zero subscripts refer to the unperturbed background. Coordinates of the velocity perturbations are given by: $\mathbf{v} = u\mathbf{e}_x + v\mathbf{e}_y + w\mathbf{e}_z$, $\Delta \mathbf{v} = \Delta u\mathbf{e}_x + \Delta v\mathbf{e}_y + \Delta w\mathbf{e}_z$. We then decompose the perturbation into axisymmetric Fourier modes $\propto \exp[i(k_x x + k_z z - \omega t)]$. Here, k_x and k_z are real wavenumbers and $\omega \equiv \omega_{\mathbb{R}} + is$ is a complex frequency, with $\omega_{\mathbb{R}}$ a wave frequency and s a growth rate (if $s < 0$, the perturbation is damped).

YG05 studied the resulting sixth-order system numerically and found unconditional instability, regardless of the value of the dimensionless parameters τ_s and f_p , with a subdynamical growth rate scaling like $\Omega \tau_s$ in the tight-coupling limit. For a given τ_s and f_p , growth was maximised in the k_x - k_z plane in a long-wavelength ridge (with $k_z \sim k_x^2 t_{\text{stop}}/(\Omega f_g)$) and a short-wavelength branch with $k_z \gg k_x$ (k_x having a preferred value). Growth was strongly suppressed in the former for dust-to-gas ratio near unity ($f_p \sim f_g \sim 0.5$). YG05 found that the wave speed $\omega_{\mathbb{R}}/k_x$ was bounded by U_{sum} defined as the sum of the background radial velocities of the dust and the gas, respectively, and growth rates (generally smaller than $|k_x|U_{\text{sum}}/2$) were maximised when the said wave speed was about $U_{\text{sum}}/2$.

2.2 Terminal velocity approximation

To gain physical insight on the streaming instability, we need some simplifications to make the problem tractable analytically. We shall adopt the “terminal velocity approximation” (YG05), that is take the left-hand-side of equation (10) to be zero, such that the relative drift is given by:

$$\Delta \mathbf{V} = \frac{\nabla P}{\rho} t_{\text{stop}}. \quad (21)$$

This approximation holds provided (i) the perturbation and dynamical timescales (ω^{-1} and Ω^{-1}) are longer than $f_g t_{\text{stop}} = \rho_s a/(\rho v_T)$ (where the equality holds in the Epstein drag regime) and (ii) the lengthscale $1/k$ of variation is longer than the “stopping length” $f_g g_e t_{\text{stop}}^2 = f_g \tau_s^2 L$ (see Appendix B for justification).

We will additionally neglect \mathbf{F} and \mathbf{G} because of the smallness of $\Delta \mathbf{V}$, an approximation YG05 find to be safe for $\omega \ll \Omega$.

The linearised system of equations is then:

$$-i\omega u - 2\Omega v + g_e \delta + ik_x h = 0 \quad (22)$$

$$\frac{\kappa^2}{2\Omega} u - i\omega v = 0 \quad (23)$$

$$-\omega w + k_z h = 0 \quad (24)$$

$$ik_x u + ik_z w - i\omega \delta = 0 \quad (25)$$

$$ik_x u + ik_z w - ik_x g_e (f_p - f_g) t_{\text{stop}} \delta + f_p k^2 t_{\text{stop}} h = 0 \quad (26)$$

where zero subscripts have been dropped, $k^2 = k_x^2 + k_z^2$, and we have introduced the epicyclic frequency κ , given by $\kappa^2 \equiv R^{-3} d(R^4 \Omega^2)/dR$. In a Keplerian disc, $\kappa = \Omega$, but one could also imagine studying streaming instabilities in any rotating fluid, possibly even by direct experimentation. Equations (22)-(24) are derived from perturbation of the x , y and z components of equation (9). Equations (25) and (26) stem from perturbing the continuity equations (7) and (8) respectively. (In equation [26] we also make use of equation [21].) Notice that the important term proportional to $(f_p - f_g)$ in equation (26) derives from a sort of buoyancy force that arises in the two fluid systems, with an effective density of ρ^2/ρ_p . When $f_p = f_g$, this effective density is stationary with respect to perturbations in ρ_p .

One can straightforwardly obtain a dispersion relation by setting the determinant of the above 5×5 system to zero¹:

$$\begin{aligned} & -if_p t_{\text{stop}} \omega^4 + \omega^3 + (if_p \kappa^2 + k_x g_e f_g) t_{\text{stop}} \omega^2 - \left(\kappa \frac{k_z}{k}\right)^2 \omega \\ & + k_x \left(\kappa \frac{k_z}{k}\right)^2 g_e t_{\text{stop}} (f_p - f_g) = 0 \end{aligned} \quad (27)$$

Series solutions in τ_s carried out by YG05 have shown that the roots fall in three branches, two epicycles giving rise to damping, and a secular mode, with:

$$\omega_{\mathbb{R}} = k_x (f_p - f_g) g_e t_{\text{stop}} + o(t_{\text{stop}}) \quad (28)$$

$$s = if_p t_{\text{stop}}^3 \left((f_p - f_g) g_e \frac{k k_x}{k_z} \right)^2 + o(t_{\text{stop}}^3), \quad (29)$$

¹ We note that the first term of the quadratic coefficient differs from that of equation (39) of YG05. While we believe that equation (27) of the current paper is correct (equation (29) corrects their equation (44) accordingly), the YG05 error appears to be typographical and in no event does it affect their exact results. Also, YG05 drop the quartic term in their equation (39); this is however consistent with $\omega t_{\text{stop}} \ll 1$.

to leading order in the stopping time². (The notation $o(X)$ indicates that the ratio $o(X)/X$ tends to zero as $X \rightarrow 0$). It can be seen that feedback is essential to the instability, as ignoring it would amount to setting $f_p = 0$ everywhere. Also, the necessity of the background drift as measured by g_e is evident. More rigorously, it may be seen that for $g_e = 0$, the dispersion relation becomes, if we disregard the $\omega = 0$ mode:

$$f_p \kappa t_{\text{stop}} X^3 - X^2 + f_p \kappa t_{\text{stop}} X - \left(\frac{k_z}{k}\right)^2 = 0 \quad (30)$$

with $X \equiv i\omega/\kappa$. One can show that, for sufficiently small κt_{stop} , this cubic has three real positive roots (in terms of X), corresponding to ω being a purely imaginary number of negative imaginary part.

2.3 The secular mode in a reduced system

It is possible to simplify the system further while retaining the leading-order physics of the instability. First, we note that, in general, $\omega \ll \Omega$, as may be judged from the exact results of YG05 or equation (28), for wavelengths that are not significantly shorter than the radial pressure scale L . Equation (23) gives us

$$u = (2i\Omega\omega/\kappa^2)v \sim (\omega/\Omega)v.$$

It is then easy to show that in equation (22) the first term (the acceleration term $-i\omega u$) can be neglected. It follows that, to leading order, the x and y equations of motion of the centre of mass relax to a form of *geostrophic balance*, i.e. Coriolis forces effectively cancel out the pressure gradient and the buoyancy force. This is important, as it means that pressure perturbations do not effectively drive centre-of-mass motions in the orbital plane. So this crucial stabilising tendency is consigned to a subdominant role. It also means that the centre of mass executes modified epicycles in the orbital plane, to leading order.

Second, we neglect the u perturbation in the two continuity equations (25) and (26) which we are permitted to do if we restrict ourselves to long radial wavelengths. From equations (22)-(23) we can obtain the following scalings

$$u \sim \frac{\omega}{\Omega} v \sim \max(k_x \frac{\omega}{\Omega^2} h, \omega \frac{g_e}{\Omega^2} \delta).$$

Combining these with (28) and equation (24), we see that $k_x u$ is subdominant here if³

$$k_x L \ll 1, \quad \text{and} \quad \left(\frac{k_x}{k_z}\right) \left(\frac{\omega}{\Omega}\right) \ll 1, \quad (31)$$

which can be satisfied if $k_x H \sim 1$ (see equation (16)) and if $k_x/k_z \lesssim 1$.

² It must be cautioned that the terminal velocity approximation discards terms of third and higher order in t_{stop} that might contribute to the leading order expansion of the *growth rate* and hence could in principle affect its sign (which the YG05 calculations show not to be the case here). Since we are here interested in understanding which ingredients give rise to instability in a model system, rather than studying its exact properties (as in YG05), we content ourselves with this heuristic approach.

³ The second condition results from requiring $k_x(k_x \omega h/\Omega^2) \ll k_z \omega$ with h eliminated from equation (24).

These approximations give us a simplified set of dynamical equations: the equations for the vertical centre of mass velocity, particle density conservation, and the incompressibility of the gas, in which drag effects enter implicitly. These are now

$$-i\omega w + ik_z h = 0 \quad (32)$$

$$ik_z w - i\omega \delta = 0 \quad (33)$$

$$ik_z w - ik_x g_e (f_p - f_g) t_{\text{stop}} \delta + f_p k^2 t_{\text{stop}} h = 0 \quad (34)$$

yielding the following quadratic dispersion relation:

$$-if_p t_{\text{stop}} \left(\frac{k}{k_z} \omega\right)^2 + \omega + k_x g_e t_{\text{stop}} (f_g - f_p) = 0, \quad (35)$$

from which we recover the secular mode and its growth rate as given in equation (29)! The corresponding eigenvector reads:

$$\begin{bmatrix} w \\ \delta \\ h \end{bmatrix} = \delta \begin{bmatrix} \omega/k_z \\ 1 \\ (\omega/k_z)^2 \end{bmatrix} \quad (36)$$

The second root corresponds to a damping $s = -(k/k_z)^2/(f_p t_{\text{stop}})$ but violates the condition $\omega t_{\text{stop}} \ll 1$ of validity of the terminal velocity approximation and will thus not be discussed further here.

It is also possible, if less rigorous, to see this reduction directly by inspection of the quartic dispersion relation (27). If we have $k_x g_e t_{\text{stop}}^2 (k_x/k_z)^2 \ll 1$ and $k_x g_e/\kappa^2 \ll 1$ (which imply the conditions of (31)), one is allowed to modify the quartic term as $-if_p t_{\text{stop}} (k/k_z)^2 \omega^4$ since $if_p (k_x/k_z)^2 t_{\text{stop}} \omega^4 \ll \omega^3$ and the quadratic one as $(if_p \kappa^2 + k_x g_e (f_g - f_p)) t_{\text{stop}} \omega^2$ since $k_x g_e f_p \ll if_p \kappa^2$. Under these conditions, the quartic may be factored as:

$$\left(\omega^2 - \left(\kappa \frac{k_z}{k}\right)^2\right) \left(-if_p t_{\text{stop}} \left(\frac{k}{k_z}\right)^2 \omega^2 + \omega + k_x g_e t_{\text{stop}} (f_g - f_p)\right)$$

such that we retrieve the quadratic dispersion relation of the reduced system.

Hence, it appears that the mathematical essence of the instability can be isolated if we make the following set of assumptions: (a) the terminal velocity approximation, in which stopping time is short and so the relative velocity is determined from the steady balance (21); (b) geostrophic balance holds in the remaining momentum equations, which account for the horizontal centre of mass velocity (the centre of mass executes modified epicycles in the orbital plane); and (c) that radial wavelengths of perturbed quantities are long (of order L or longer). In so doing, we have reduced the order of the system from 6 to 2.

The ingredients for instability, apparently, are: a vertical velocity generated by a vertical pressure gradient (equation [32]); accumulation of particles by the associated vertical flux of background particles (equation [33]); and finally gas incompressibility (equation [34]). This last equation, though difficult to interpret, is also the location that drag forces appear explicitly, via (21). Lastly, we emphasise again the importance of geostrophic balance, which offsets pressure gradients by Coriolis circulation, rather than radial flow. Thus radial pressure gradients do not drive stabilising

radial motions which might alleviate the self-same gradients (but note that vertical pressure gradients remain in full). Therefore, rotation may not make an explicit appearance in these equations but its influence is crucial, as the next section demonstrates.

3 STREAMING STABILITY IN THE ABSENCE OF ROTATION

To emphasise the importance of rotation, and geostrophic balance in particular, let us consider the same problem with neither Coriolis force nor background shear, that is, in a nonrotating frame, a uniform flow of both dust and fluid, drifting relative to each other because of a pressure gradient, which is compensated for by an external gravitational field (and/or an inertial, non-Coriolis acceleration). It is actually more straightforward to handle this problem directly in terms of the dust and solid perturbations, with none of the approximations used in §3. We denote by $\mathbf{v}_{p,g}$ the perturbations of $\mathbf{V}_{p,g}$, $\delta_p \equiv \delta/f_p$ the logarithmic density perturbation of the gas, and $h_g \equiv h/f_g$.

Perturbing equations (1)-(4) (with $\Omega = 0$), still assuming incompressibility, gives the following system:

$$(-i(\omega - \mathbf{k} \cdot \mathbf{V}_p) + \frac{1}{t_{\text{stop}}})\mathbf{v}_p - \frac{1}{t_{\text{stop}}}\mathbf{v}_g = 0 \quad (37)$$

$$-\frac{\epsilon}{t_{\text{stop}}}\mathbf{v}_p + (-i(\omega - \mathbf{k} \cdot \mathbf{V}_g) + \frac{\epsilon}{t_{\text{stop}}})\mathbf{v}_g - \frac{\epsilon}{t_{\text{stop}}}\delta_p(\mathbf{V}_p - \mathbf{V}_g) + ih_g\mathbf{k} = 0 \quad (38)$$

$$i\mathbf{k} \cdot \mathbf{v}_p - i\omega\delta_p = 0 \quad (39)$$

$$i\mathbf{k} \cdot \mathbf{v}_g = 0 \quad (40)$$

where $\epsilon \equiv \rho_p/\rho_g$, identity matrix. Setting the determinant of the above 8×8 system to zero, the following dispersion relation results:

$$\left(\omega - \mathbf{k} \cdot \mathbf{V}_p + \frac{i}{t_{\text{stop}}}\right) \left(\omega^2 + \left(\frac{i}{f_g t_{\text{stop}}} - \mathbf{k} \cdot (\mathbf{V}_p + \mathbf{V}_g)\right)\omega + (\mathbf{k} \cdot \mathbf{V}_p)(\mathbf{k} \cdot \mathbf{V}_g) - i\frac{\mathbf{k} \cdot \mathbf{V}}{f_g t_{\text{stop}}}\right)^2 = 0 \quad (41)$$

The first factor corresponds to a mode where the gas' velocity field is unperturbed, with the gas compensating the disturbance of the dust's with variation of pressure and density. The quadratic factor (squared) has roots:

$$\omega = \frac{1}{2} \left(\mathbf{k} \cdot (\mathbf{V}_p + \mathbf{V}_g) + \frac{i}{f_g t_{\text{stop}}} \left(-1 \pm \sqrt{(1 + i(\epsilon - 1)(f_g t_{\text{stop}})^2 \mathbf{k} \cdot \mathbf{g}_e)^2 - 4\epsilon(\mathbf{k} \cdot \mathbf{g}_e(f_g t_{\text{stop}})^2)^2} \right) \right), \quad (42)$$

with $\mathbf{g}_e \equiv \nabla P/\rho$. Using the lemma $|\text{Re}(\sqrt{(1+ia)^2 - b^2})| \leq 1$ for $(a, b) \in \mathbb{R}^2$ (YG05), their imaginary part (s) is always negative. For $\mathbf{k} \cdot \mathbf{g}_e(f_g t_{\text{stop}})^2 \ll 1$ (as in the terminal velocity approximation limit), these roots may be expanded as

$$\mathbf{k} \cdot (f_p \mathbf{V}_g + f_g \mathbf{V}_p) - i\epsilon(\mathbf{k} \cdot \mathbf{g}_e)^2(f_g t_{\text{stop}})^3 \quad (43)$$

and

$$\mathbf{k} \cdot \mathbf{V} - \frac{i}{f_g t_{\text{stop}}} \quad (44)$$

the latter corresponding to a damping where dust and fluid converge in concert toward equilibrium.

There is thus no streaming instability in the absence of rotation (as was also clear from the YG05 numerical calculations). Rotation, as well as feedback, are both essential for the streaming instability, hence the difficulty in finding a simple toy model to explain it.

4 TOWARD AN INTERPRETATION OF THE STREAMING INSTABILITY

We now develop a framework with which to interpret the streaming instability.

4.1 Particle concentration in pressure maxima

We start with the equation governing the evolution of the dust mass fraction. Combining equations (1) and (2) (we use here the full equations rather than those of the reduced system), we obtain:

$$\mathcal{D}_p \ln \frac{\rho_p}{\rho} + \frac{\nabla \cdot (\rho_g(\mathbf{V}_p - \mathbf{V}_g))}{\rho} = 0. \quad (45)$$

It is clear from this equation that dust is advected by \mathbf{V}_p but is also subject to a mass flux associated with the relative drift (the second term on the left-hand-side of equation (45)). We might expect then to observe dust clumps correlated with $\Delta \mathbf{V}$ (as noted by YG05 in the caption of their figure 6). In the terminal velocity approximation, equation (45) becomes:

$$\begin{aligned} \mathcal{D}_p \ln \frac{\rho_p}{\rho} &= -\frac{1}{\rho} \nabla \cdot \left(\rho_g t_{\text{stop}} \frac{\nabla P}{\rho} \right) \\ &= \frac{\rho_g}{\rho} \left(\Delta \mathbf{V} \cdot \nabla \ln \rho - t_{\text{stop}} \frac{\nabla^2 P}{\rho} \right), \end{aligned} \quad (46)$$

where the latter equality assumes the constancy of $\rho_g t_{\text{stop}}$. There are two terms on the right-hand-side: one due to density variation, and one to pressure variation. We shall show below that the latter is responsible for growth, not the former (as was also ruled out by YJ07). Equation (46) may be rewritten in the useful form:

$$\left(\frac{\partial}{\partial t} + (f_p \mathbf{V}_g + f_g \mathbf{V}_p) \cdot \nabla \right) \ln \frac{\rho_p}{\rho} = -\frac{\rho_g t_{\text{stop}}}{\rho^2} \nabla^2 P \quad (47)$$

in which we have used incompressibility. Note that we have not yet linearised the system—this equation holds equally well in the nonlinear regime—and also that in this subsection we have made no hypothesis on the centre of mass dynamics (e.g. presence of Coriolis forces), since we have only used mass conservation equations and the terminal velocity approximation. Its linearised form, however, with the Fourier dependence $\exp[i(k_x x + k_z z - \omega t)]$, yields

$$\omega = \mathbf{k} \cdot (f_p \mathbf{V}_g + f_g \mathbf{V}_p) + i f_p k^2 t_{\text{stop}} \frac{P'}{\rho'_p}, \quad (48)$$

with $P' \equiv \rho h$ and $\rho'_p \equiv \rho \delta$ the perturbation in pressure and (particle) density, respectively.

What we have in (47) is a form of 'advective-reaction' equation. Dust is advected at a velocity intermediate between \mathbf{V}_p and \mathbf{V}_g , to wit

$$f_p \mathbf{V}_g + f_g \mathbf{V}_p = \mathbf{V}_p + (\mathbf{V}_g - \mathbf{V}) \quad (49)$$

which corresponds to the U_{sum} of YG05, as in the frame used, $\mathbf{k} \cdot \mathbf{V} = 0$. On the right hand side we have a source term proportional to the pressure Laplacian. This term will tend to draw dust *towards* pressure maxima in the $x - z$ plane and *away* from pressure minima. Clearly, instability is intimately connected with this term, and the unstable mode works by concentrating dust at pressure maxima. We discuss both processes in turn.

4.2 Advection term

The left-hand side of equation (47) gives rise to the streaming instability wave character: a density pattern in x and z will be advected at the velocity

$$\mathbf{V}_p + (\mathbf{V}_g - \mathbf{V}) \quad (50)$$

and in the linear regime this will be entirely radial. The advection velocity is the sum of two parts: the particle velocity and a secondary contribution issuing from the relative drag (the bracketed term). The first term should be familiar, and simply describes the Lagrangian advection of particles by the particle velocity itself. The second term is novel. Physically, it represents the fact that particle density maxima induce a *decrease* in the relative velocity - because the reciprocal drag of the two fluids is greater at that location (cf. the first term in equation [10]). This decrease leads to an additional mass flux, which is anticorrelated with ρ'_p . An outward effective advection is the result, which is in addition (and opposition) to that of \mathbf{V}_p . Thus a density peak will tend to be both (a) pushed inward simply by the primary particle velocity \mathbf{V}_p , and (b) pushed outward by the second drag-induced mass flux that it has itself excited. It is easy to show that for $f_g = f_p$ the sum of the two velocities is precisely zero, i.e. the two drift velocities cancel perfectly. Conversely, when there are very few particles, i.e. $f_p \rightarrow 0$, the advection velocity is simply \mathbf{V}_p and the pattern is carried by the particle fluid alone. This is because, in this limit, the particles' influence on the gas is so minor that \mathbf{V}_g is effectively zero. On the other hand, when there is virtually no gas, $f_g \rightarrow 0$, the advection approaches zero, because $\mathbf{V}_g \rightarrow 0$ (as well as \mathbf{V}_p) in this limit.

4.3 Instability term

We have already mentioned that instability was related to pressure maxima (or technically, pressure *perturbation* maxima, as there is a background gradient, which however has zero Laplacian). This is reminiscent of the concentration mechanism of test particles in long-lived, two-dimensional vortices (e.g. Barge and Sommeria 1995; Klahr and Bodenheimer 2006), which in a Keplerian flow are anticyclonic.

In the streaming instability, this concentration is an active process, in the sense that feedback participates in the preservation of the high-pressure, particle-trapping zones. How does the instability grow? Schematically, as we have said, pressure maxima attract dust particles, as can be seen from the terminal velocity approximation given by equation (21). Then, dust drags the gas toward these same maxima (see the gas Euler equation (4), where the terminal velocity approximation (21) may be injected). This creates convergent flows that *strengthen* these pressure maxima. These in

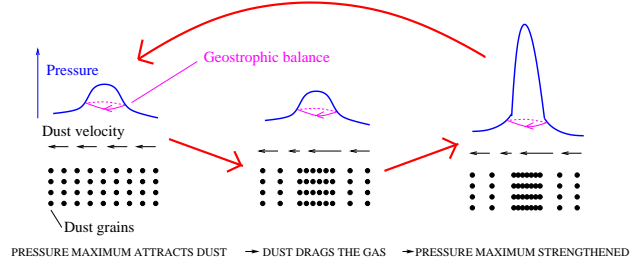


Figure 1. Cartoon of the proposed interpretation of the streaming instability (seen along the radial axis). Dust is drifting radially inward. The pressure profile is drawn in blue (we ignore the background gradient in the picture). We start with a pressure perturbation maximum. This attracts dust, which in turn drags the gas, creating convergent flows that strengthen the pressure maximum. Note the role of geostrophic balance in maintaining a circulation (schematically shown in magenta) which supports the pressure maximum.

turn can attract more dust particles, and the process thus runs away. This is sketched in Figure 1.

Indeed, inspection of equation (48) shows that growth is correlated with $f_p P' / \rho'_p$. f_p is a measure of the feedback of dust on the gas, while P' / ρ'_p measures how well dust density and pressure maxima correlate with each other, or in other words, the efficiency of the dust-driven pressure loading. Growth is positive if both pressure and density perturbations are not out of phase by more than 90° . For example, YJ07's eigenvector “linA” has a pressure phase relative to particle density of 43° and a complex frequency $\omega = (-0.3480127 + 0.4190204i)\Omega$ while that same phase for “linB” is -95° with a complex frequency $\omega = (0.4998786 + 0.0145764i)\Omega$.⁴ For the secular mode in the reduced model, $P' / \rho'_p = h / \delta = (\omega / k_z)^2$ (see equation (36)) is real and positive to leading order.

While the above identifies the positive feedback loop leading to instability, we have yet to account for two other physical ingredients that are necessary condition to it. Indeed, drag of the dust on the gas is actually insufficient alone to offset the pressure force that tends to accelerate gas *away* from pressure maxima. In the terminal velocity approximation, we have:

$$\frac{\rho_p}{\rho_g} \frac{\mathbf{V}_p - \mathbf{V}_g}{t_{\text{stop}}} - \frac{\nabla P}{\rho_g} = - \frac{\nabla P}{\rho}, \quad (51)$$

The first physical ingredient we wish to mention is rotational dynamics, whose necessity has been shown in §3. We have already mentioned in §2.3 that a geostrophic balance is established, by which Coriolis forces essentially balance the pressure force. The other physical ingredient is the background solid-to-gas drift (due to the pressure gradient), as noted in §2.2. Mathematically, a nonzero drift is required for particle density to affect the dynamics, as, in the reduced system, this can only happen through the “buoyancy force term” (proportional to the pressure gradient) in the gas continuity equation (8) as mentioned in §2.2, which contributes to the advection term discussed in §4.2. We suggest

⁴ s is slightly positive, instead of slightly negative, presumably because of finite gas compressibility and/or corrections to the terminal velocity approximation.

that the physical explanation for this is that relative drift between the pressure maximum and the dust allows the former to sweep a (radial) “headwind” of particles and be an effective “trap” for the dust.

We note that the processes discussed in the previous paragraph are restricted to the x - y plane and emphasise radial drifts and gradients. The fact that the reduced model seems to emphasise vertical gradients—although the leading-order growth rate given by equation (29) is negatively correlated with k_z —may be interpreted as resulting from incompressibility, as radial velocity perturbations of the gas must then give rise to vertical perturbations and gradients (see e.g. flow pattern in Fig. 5 of YG05).

4.4 Streaming instability as collective drag?

The above demonstration leads us to question the correspondence suggested by CY10 between the streaming instability and the toy model of Goodman and Pindor (2000), which was originally designed for a dust layer-scale instability. In this one-dimensional, single-fluid model, the acceleration is the sum of g , a proxy for gravity, pressure and inertial forces, and $-\nu_d(\Sigma)v$ a density-dependent drag acceleration proportional to the velocity v of the fluid. As long as $d\nu_d/d\Sigma \neq 0$, linear analysis shows the system to be overstable (CY10).

The fact that this toy model is one-dimensional appears to prevent it from capturing the specificities of Coriolis forces, unlike other gravitational or inertial terms. It may also be questionable whether in the linear phase, and in the local treatment of the instability, the drag can be considered to be collective in the sense of the above toy model, and what would play the role of the (single) fluid of this model. Certainly, the latter cannot be the gas+dust fluid, as drag is internal to it (see equation [9]). But even if we take the dust for example, and use the terminal velocity approximation (or higher-order corrections) as a proxy to eliminate the gas velocity (we cannot treat it as *imposed*—this is indeed the point of the streaming instability), the drag acceleration becomes $-\nabla P/\rho$ which makes no reference to the dust velocity. Same holds for the gas. Finally, as we have noted earlier, the variation of the relative drift with density is not responsible for growth in this approximation and hence does not conform to the notion of a collective drag underlying the instability.

5 CONCLUSION

Through successive approximations, we have obtained a reduced system giving rise to the streaming instability. It would appear that the essence of the instability can be effectively established given:

- the terminal velocity approximation
- that a form of geostrophic balance holds for the planar centre of mass velocity
- that radial wavelengths are sufficiently long.

The leading order (in the stopping time) expansion of the growth rate is the same as the fourth-order system with the terminal velocity approximation.

We interpret the streaming instability as arising from dust pileup in pressure perturbation maxima, with the dust then dragging the gas and hence strengthening the maxima. For this enhancement process to occur despite the pressure force that tends to “smear” these maxima out, it is necessary that there be a background solid-gas drift, and also Coriolis forces that help establish a geostrophic balance with the pressure force. The role of Coriolis forces would appear to indicate that one-dimensional toy models do not adequately capture the instability.

Larger amplitude vertical flows will (when outside of the linear regime) transport density away from maxima and hence limit the growth of the instability. and would compete with other nonlinear effects like particle clumping (‘traffic jams’). Incidentally, another process in the nonlinear saturation that will work against particle clumping is particle pressure, not usually modelled. The large local densities of nonlinear clumps will lead to enhanced collision frequencies and consequently to a particle pressure which will resist further concentration. Attempts to establish the conditions for self-gravitational collapse of such clumps should in principle include this effect.

REFERENCES

- Bai, X. and Stone, J. M. (2010). Particle-gas Dynamics with Athena: Method and Convergence. *ApJS*, **190**, 297–310.
- Balbus, S. A. and Hawley, J. F. (1998). Instability, turbulence, and enhanced transport in accretion disks. *Reviews of Modern Physics*, **70**, 1–53.
- Barge, P. and Sommeria, J. (1995). Did planet formation begin inside persistent gaseous vortices? *A&A*, **295**, L1–L4.
- Chiang, E. (2008). Vertical Shearing Instabilities in Radially Shearing Disks: The Dustiest Layers of the Protoplanetary Nebula. *ApJ*, **675**, 1549–1558.
- Chiang, E. and Youdin, A. N. (2010). Forming Planetesimals in Solar and Extrasolar Nebulae. *Annual Review of Earth and Planetary Sciences*, **38**, 493–522.
- Cuzzi, J. N., Davis, S. S., and Dobrovolskis, A. R. (2003). Blowing in the wind. II. Creation and redistribution of refractory inclusions in a turbulent protoplanetary nebula. *Icarus*, **166**, 385–402.
- Dominik, C., Blum, J., Cuzzi, J. N., and Wurm, G. (2007). Growth of Dust as the Initial Step Toward Planet Formation. *Protostars and Planets V*, pages 783–800.
- Epstein, P. S. (1924). On the resistance experienced by spheres in their motion through gases. *Phys. Rev.*, **23**(6), 710–733.
- Fleming, T. and Stone, J. M. (2003). Local Magnetohydrodynamic Models of Layered Accretion Disks. *ApJ*, **585**, 908–920.
- Gammie, C. F. (1996). Layered Accretion in T Tauri Disks. *ApJ*, **457**, 355–.
- Garaud, P., Barrière-Fouchet, L., and Lin, D. N. C. (2004). Individual and Average Behavior of Particles in a Protoplanetary Nebula. *ApJ*, **603**, 292–306.
- Goldreich, P. and Ward, W. R. (1973). The Formation of Planetesimals. *ApJ*, **183**, 1051–1062.
- Goodman, J. and Pindor, B. (2000). Secular Instability

- and Planetesimal Formation in the Dust Layer. *Icarus*, **148**, 537–549.
- Ida, S. (2010). Planet formation from planetesimals and diversity of planetary systems. In T. Montmerle, D. Ehrenreich, & A.-M. Lagrange, editor, *EAS Publications Series*, volume 41 of *EAS Publications Series*, pages 339–354.
- Johansen, A. and Youdin, A. (2007). Protoplanetary Disk Turbulence Driven by the Streaming Instability: Nonlinear Saturation and Particle Concentration. *ApJ*, **662**, 627–641.
- Johansen, A., Oishi, J. S., Mac Low, M., Klahr, H., Henning, T., and Youdin, A. (2007). Rapid planetesimal formation in turbulent circumstellar disks. *Nature*, **448**, 1022–1025.
- Klahr, H. and Bodenheimer, P. (2006). Formation of Giant Planets by Concurrent Accretion of Solids and Gas inside an Anticyclonic Vortex. *ApJ*, **639**, 432–440.
- Latter, H. N., Bonart, J. F., and Balbus, S. A. (2010). Resistive double-diffusive instability in the dead zones of protostellar discs. *MNRAS*, **405**, 1831–1839.
- Lee, A. T., Chiang, E., Asay-Davis, X., and Barranco, J. (2010a). Forming Planetesimals by Gravitational Instability. I. The Role of the Richardson Number in Triggering the Kelvin-Helmholtz Instability. *ApJ*, **718**, 1367–1377.
- Lee, A. T., Chiang, E., Asay-Davis, X., and Barranco, J. (2010b). Forming Planetesimals by Gravitational Instability. II. How Dust Settles to its Marginally Stable State. *ApJ*, **725**, 1938–1954.
- Lesur, G. and Papaloizou, J. C. B. (2010). The subcritical baroclinic instability in local accretion disc models. *A&A*, **513**, A60+.
- Nakagawa, Y., Sekiya, M., and Hayashi, C. (1986). Settling and growth of dust particles in a laminar phase of a low-mass solar nebula. *Icarus*, **67**, 375–390.
- Weidenschilling, S. J. (1977). Aerodynamics of solid bodies in the solar nebula. *MNRAS*, **180**, 57–70.
- Weidenschilling, S. J. (1980). Dust to planetesimals - Settling and coagulation in the solar nebula. *Icarus*, **44**, 172–189.
- Youdin, A. and Johansen, A. (2007). Protoplanetary Disk Turbulence Driven by the Streaming Instability: Linear Evolution and Numerical Methods. *ApJ*, **662**, 613–626.
- Youdin, A. N. (2011). On the Formation of Planetesimals Via Secular Gravitational Instabilities with Turbulent Stirring. *ApJ*, **731**, 99+.
- Youdin, A. N. and Goodman, J. (2005). Streaming Instabilities in Protoplanetary Disks. *ApJ*, **620**, 459–469.
- Zsom, A., Ormel, C. W., Güttler, C., Blum, J., and Dullemond, C. P. (2010). The outcome of protoplanetary dust growth: pebbles, boulders, or planetesimals? II. Introducing the bouncing barrier. *A&A*, **513**, A57+.

APPENDIX A: APPROXIMATING DUST AS A PRESSURELESS FLUID COUPLED TO THE GAS

It is of interest to investigate in some generality how the description of dust as a pressureless fluid, used in many simulations, arises. As CY10 point out, the usual criteria for gas molecules do not apply. Intuitively, one expects a fluid description to be viable if the stopping time is short

in some sense (YG05, see also YJ07). Here, we verify this intuition using a kinetic approach. Garaud *et al.* (2004) addressed this problem for one-dimensional settling in a static, homogeneous gas, finding that velocity dispersion would be quickly damped for tightly coupled particles in the Epstein regime.

We introduce a distribution function $f(\mathbf{r}, \mathbf{v}_p)$ of the number of particles in the $(\mathbf{r}-\mathbf{v}_p)$ phase space. The continuity equation in this space may be written as:

$$\frac{\partial f}{\partial t} + \mathbf{v}_p \cdot \frac{\partial f}{\partial \mathbf{r}} + \frac{\partial}{\partial \mathbf{v}_p} \cdot \left(f \frac{\mathbf{F}_p}{m_p} \right) = I_{\text{coll}}, \quad (\text{A1})$$

with \mathbf{F}_p the total force exerted on one particle (except particle-particle interactions), m_p the particle mass and I_{coll} the collision integral. We have used $\frac{\partial}{\partial \mathbf{r}} \cdot (f \mathbf{v}_p) = \mathbf{v}_p \cdot \frac{\partial f}{\partial \mathbf{r}}$ but here, $\frac{\partial}{\partial \mathbf{v}_p} \cdot \mathbf{F}_p \neq 0$ because \mathbf{F}_p includes the drag force $-m_p(\mathbf{v}_p - \mathbf{V}_g)/t_{\text{stop}}$, hence the departure of the left-hand-side from the standard Boltzmann equation form⁵.

Provided collisions conserve the total number and momentum of particles, integration over velocities of equation (A1) multiplied by \mathbf{v}_p , yields:

$$\mathcal{D}_p \mathbf{V}_p = \frac{1}{m_p} \langle \mathbf{F}_p \rangle - \frac{1}{\rho_p} \nabla \cdot \mathbf{S}, \quad (\text{A2})$$

with $\mathbf{V}_p = \langle \mathbf{v}_p \rangle$ the mean particle velocity, $\mathbf{S} \equiv \rho_p \langle (\mathbf{v}_p - \mathbf{V}_p)(\mathbf{v}_p - \mathbf{V}_p) \rangle$ the stress tensor. For any particle-wise quantity x , we have defined:

$$\langle x \rangle \equiv \frac{m_p}{\rho_p} \int x f d^3 \mathbf{v}_p. \quad (\text{A3})$$

Treating the dust as a pressureless fluid amounts to neglecting the stress tensor in equation (A2). To evaluate this, it is of interest to derive its evolution equation:

$$\begin{aligned} \mathcal{D}_p S^{ij} = & m_p \int I_{\text{coll}} (v_p^i - V_p^i)(v_p^j - V_p^j) d^3 \mathbf{v}_p \\ & - \int \left(F_p^i (v_p^j - V_p^j) + F_p^j (v_p^i - V_p^i) \right) f d^3 \mathbf{v}_p \\ & - m_p \int (\mathbf{v}_p - \mathbf{V}_p) \cdot \frac{\partial f}{\partial \mathbf{r}} (v_p^i - V_p^i)(v_p^j - V_p^j) d^3 \mathbf{v}_p. \end{aligned} \quad (\text{A4})$$

The first term on the right-hand-side relates to the redistribution and loss of relative velocities during collisions, the second to the action of velocity-dependent forces, and the third to transport of velocity dispersion between neighbouring “fluid elements”. The drag contribution to the second term is $-2S^{ij}/t_{\text{stop}}$ (for a velocity-independent t_{stop}).

In the absence of particle-particle interaction ($I_{\text{coll}} = 0$), integration over space of equation (A4) yields:

$$\begin{aligned} \frac{d}{dt} \langle S^{ij} \rangle_V = & -2 \langle \frac{S^{ij}}{t_{\text{stop}}} \rangle_V - \left(\epsilon_{ikl} \Omega^l \langle S^{kj} \rangle_V + \langle \frac{\partial V_p^i}{\partial x^k} S^{kj} \rangle_V \right. \\ & \left. + \epsilon_{jkl} \Omega^l \langle S^{ki} \rangle_V + \langle \frac{\partial V_p^j}{\partial x^k} S^{ki} \rangle_V \right) \end{aligned} \quad (\text{A5})$$

$\langle \dots \rangle_V$ denotes a spatial averaging. ϵ_{ijk} is the Levi-Civita tensor and Ω is the instantaneous rotation vector of the reference frame. Damping by gas drag dominates the evolution of the velocity dispersion if t_{stop} is shorter than Ω^{-1} and the

⁵ Thus, technically, what Garaud *et al.* (2004) called an interaction term, although their approach was collision-free, actually is the corresponding correction to the left-hand side.

viscous heating rate $|\nabla \mathbf{V}_p|^{-1}$. This is thus the criterion for validity of the pressureless fluid approximation.

APPENDIX B: VALIDITY OF THE TERMINAL VELOCITY APPROXIMATION

Perturbing equation (10) yields:

$$\begin{aligned} & -i\omega\Delta\mathbf{v} - 2\Omega\Delta v\mathbf{e}_x + \frac{\Omega}{2}\Delta u\mathbf{e}_y \\ & -ik_x g_e t_{\text{stop}} (\mathbf{v} + (f_g - f_p)\Delta\mathbf{v} - f_g\Delta\mathbf{V}\delta) \\ & = -\frac{\Delta\mathbf{v} + \delta\Delta\mathbf{V}}{f_g t_{\text{stop}}} + i\frac{h}{f_g}\mathbf{k} \end{aligned} \quad (\text{B1})$$

(This can also be obtained by injecting equation 31 into equation 27 of YG05). The terminal velocity approximation amounts to setting the left-hand-side equal to zero.

The constraint $\omega f_g t_{\text{stop}} \ll 1$ results from comparing the first term on the left-hand-side with the first one on the right-hand-side. The latter dominates the next two terms on the left-hand-side if $\Omega f_g t_{\text{stop}} \ll 1$, and the fourth and fifth ones if $f_g k_x g_e t_{\text{stop}}^2 \ll 1$ (recall that both f_p and f_g are smaller than 1). To justify the assertion for the fourth term, we combine the perturbations of (7) and (8) (equations 28 and 29 of YG05) to obtain:

$$\mathbf{k} \cdot \mathbf{v} = \frac{f_p \mathbf{k} \cdot \Delta\mathbf{v}}{1 + \frac{f_g k_x g_e t_{\text{stop}}}{\omega}} \quad (\text{B2})$$

and use the expectation that the wave speed is of order the background drift velocity, as verified by YG05.⁶ The final term on the left-hand-side is dominated by the second one on the right-hand-side under the same condition.

The condition $f_g t_{\text{stop}} \ll \Omega^{-1}, \omega^{-1}$ is implied anyway for the validity of the fluid approximation (see Appendix A). Since $\omega < \Omega$, the condition on τ_s ($\ll 1/f_g$) is the most stringent one. These conditions are somewhat less stringent than those mentioned by YG05 (which are thus sufficient), and more symmetric with respect to dust and gas (as they converge in concert toward the terminal (relative drift) velocity because of their mutual interaction).

⁶ Actually, equation (B2) does not really constrain v , but if we adopt the scaling $v \sim \frac{\Omega}{\omega}u$ from equation (23), the condition for this component reduces to the already obtained $\Omega f_g t_{\text{stop}} \ll 1$.